

Polymer Chemistry

Accepted Manuscript



This is an *Accepted Manuscript*, which has been through the Royal Society of Chemistry peer review process and has been accepted for publication.

Accepted Manuscripts are published online shortly after acceptance, before technical editing, formatting and proof reading. Using this free service, authors can make their results available to the community, in citable form, before we publish the edited article. We will replace this *Accepted Manuscript* with the edited and formatted *Advance Article* as soon as it is available.

You can find more information about *Accepted Manuscripts* in the [Information for Authors](#).

Please note that technical editing may introduce minor changes to the text and/or graphics, which may alter content. The journal's standard [Terms & Conditions](#) and the [Ethical guidelines](#) still apply. In no event shall the Royal Society of Chemistry be held responsible for any errors or omissions in this *Accepted Manuscript* or any consequences arising from the use of any information it contains.

ARTICLE

Nano-Building Blocks based-Hybrid organic-inorganic copolymers with Self-Healing Properties.

Cite this: DOI: 10.1039/x0xx00000x

F. Potier,^{a,b,c} A. Guinault,^d S. Delalande,^e C. Sanchez,^{a,b,c} F. Ribot^{a,b,c} and L. Rozes^{a,b,c} *

Received 00th January 2012,
Accepted 00th January 2012

DOI: 10.1039/x0xx00000x

www.rsc.org/

New dynamic materials, that can repair themselves after a strong damage, have been designed by hybridization of polymers with structurally well-defined nanobuilding units. The controlled design of cross-linked poly(*n*-butyl acrylate) (pBuA) has been performed by introducing a very low amount of a specific tin oxo-cluster. Sacrificial domains with non-covalent interactions (*i.e.* ionic bonds) developed at the hybrid interface play a double role. Such interactions are strong enough to cross-link the polymer, which consequently exhibits rubber-like elasticity behavior and labile enough to enable, after a severe mechanical damage, dynamic bond recombination leading to an efficient healing process at room temperature. In agreement with the nature of the reversible links at the hybrid interface, the healing process can be speed up considerably with temperature. ¹H and ¹¹⁹Sn PFG NMR has been used to evidence the dynamic nature of these peculiar cross-linkings nodes.

Introduction

Over the last decade, a broad range of self-healing materials has emerged.¹⁻³ Such systems, when they have been damaged, heal themselves either spontaneously or with the aid of a stimulus. Several of these materials draw their inspiration from the design of biological materials.⁴ As an example, the bio-reparation of mussel byssal threads proceeds by the reconnection after damage of sacrificial cross-links constituted by clustered distribution of catecholato-iron chelate complexes distributed in a polymeric scaffold.^{5,6} On the other hand, hybrid materials or nanocomposites, defined as composites constituted of two components, one inorganic and the other one organic in nature mixed at the nanometer level, have attracted strong interest both in academia and industry.^{7,8} The combination at the nanoscale of organic and inorganic components leads to high homogeneous materials which develop extended organic-inorganic interfaces with tuneable chemical organic-inorganic bonds from weak to strong interactions. The accurate control of the hybrid interfaces does not only lead to the developments of multiscale porous materials or bio-inspired nanomaterials but also leads to the adjustment of a large set of properties (optical, mechanical, separation capacity, catalysis, chemical and thermal stability).⁹⁻¹³

Among the different strategies to design hybrid materials, the modular approach, which assembles well-defined Nano-Building Blocks, NBBs, (nanoparticles or clusters), into macroscopic networks, presents several advantages.¹⁴⁻¹⁹ The

step-by-step development of the material allows to better control the structure at the nanometer scale; especially the perfect monodispersity of oxo-clusters allows the development of well-defined structures and leads to an enhanced quality in the final material.^{20,21} For several hybrids constructed *via* a “legolike” chemistry, the structural relations between the NBBs and the polymeric matrix has been studied during the past decades. An analysis of this literature, suggests that well-defined monodispersed metallic oxo-clusters, are appropriate candidates to design new hybrid organic-inorganic materials that can provide interesting and original alternative to obtain efficient and up-scalable self-healing materials.

In the context of self-healing materials, repairing a mechanical damage need the generation of a dynamic phase combined with the presence of peculiar chemical bonds able to be reversibly exchanged and redistributed in order to close the crack.¹⁻³ Focusing on such prerequisite, we propose a novel strategy based on the preparation of elastomeric nanocomposites from a cheap and common organic monomer copolymerized with metallic oxo-clusters. Indeed, the small size of the inorganic component and the elastomeric behavior of the host matrix have been selected to facilitate matter transport towards the damage site. Moreover, the key parameter to reach the expected property is a fine-tuning of the nature of the hybrid interface, achieved by the choice of organic ligands, which surround the metallic oxo-core of clusters. Subsequently, a hybrid interface based on ionic interactions as sacrificial cross-links has been investigated to prepare dynamic systems and ease the

subsequent reconnection of local bonds after damage. To the best of our knowledge, no healing properties have ever been reported on the NBBs approach using available polymers cross-linked by ionic bonds.

Results and discussion

A butyltin oxo-cluster macrocation, $[(\text{BuSn})_{12}\text{O}_{14}(\text{OH})_6]^{2+}$, functionalized with two 2-acrylamido-2-methyl-1-propanesulfonate anions (AMPS),²² has been chosen both as a cross-linking agent and a healing agent. The hybrid character of the NBB, and especially the presence of butyl moieties at the surface of the inorganic core enable its easy dissolution in *n*-butyl acrylate (BuA) without the need of additional solvent. Polymerization of the mixture is achieved by a conventional thermal radical polymerization procedure using AIBN (Azobisisobutyronitrile) as initiator. Figure 1 presents a schematic of material preparation. Such a bottom up strategy leads to the easy preparation of transparent homogeneous coatings or monolithic samples with no limitation of the size of the samples.

Figure 1. Schematic representation of the hybridization of the polymer by the butyltin oxo-cluster macrocation, $[(\text{BuSn})_{12}\text{O}_{14}(\text{OH})_6]^{2+}$, functionalized through ionic interactions with two charge compensating acrylamido anions.

First, FTIR and NMR analysis demonstrate that the presence of the NBBs does not affect the conversion of monomer to polymer by the total disappearance of the signals of vinylic groups expected at 1630 cm^{-1} on the IR spectrum and 5,5-6,5 ppm and 125-135 ppm on the ^1H and ^{13}C NMR spectra, respectively. The permanence of the network was confirmed by carrying out swelling experiments. The hybrid sample swells, but does not dissolve, when it is immersed at room temperature in poorly dissociating solvent such as chloroform (dielectric constant, $\epsilon = 4.81$). On the contrary, in highly dissociating solvents, such as *N,N*-dimethylformamide ($\epsilon = 36.7$), the sample loses its integrity, in agreement with the ionic nature of the links that create the network. Furthermore, the integrity of the NBB is preserved and randomly distributed inside the copolymerized network. Indeed, the solution ^{119}Sn -(^1H) NMR spectrum of a piece of material swollen with CDCl_3 displays the two characteristic resonances of the butyltin oxo-cluster (Figure S11), *ie.* a first one at -283 and a second one at -463 ppm, which correspond to the five and six-coordinated tin atoms, respectively. Compared to the resonances commonly observed in solutions for $[(\text{BuSn})_{12}\text{O}_{14}(\text{OH})_6]\text{X}_2$ compounds, the ones observed in the swollen network are clearly broadened. This feature is in line with the node nature of the macrocation, which strongly reduces its tumbling rate and, therefore, decreases the T_2 relaxation times. In such species, the relaxation is mostly related to chemical shift anisotropy (CSA) and indeed the broadening is more important for the CSnO_4 environment, which exhibits a larger CSA.^{22, 23}

DSC, DMTA and tensile strength measurements have been performed to determine the mechanical characteristics of the polymer nanocomposite. For comparison, a covalently cross-linked pBuA has been prepared by copolymerization of *n*-BuA with an organic covalent cross-linker (1,6 hexanediol dimethacrylate). The very moderate increase of the glass transition temperature (T_g) on DSC thermograms from -50°C for the neat polymer to -46°C for the pBuA cross-linked by covalent bonds (0.6 wt%), and -49°C for the hybrid pBuA cross-linked by ionic bonds (2 wt% of tin oxo-clusters), demonstrates that the cross-linking of the polymer chains does not prevent the cooperative motion of chain segments. Figure 2a displays the storage modulus (E') as a function of temperature of the samples with covalent and ionic cross-linkers. In both cases, a strong decrease of the modulus is observed at the glass transition, followed by a rubbery plateau highlighted the rubbery elasticity behavior of the samples. At room temperature, the cross-linked hybrid network behaves like an elastomer. It has a modulus in the rubbery state of 0.26 MPa and a high elongation at break was determined by tensile strength measurement (higher than 1800%).

When the monolithic hybrid sample is broken into pieces and when the pieces are replaced together at room temperature, the recovery of the integrity of the sample is clearly observed and illustrated in figure 3. By increasing the time of contact at room temperature and also by the achievement of a thermal treatment the recovery of the aspect and properties (tensile strength and elongation at break) of the sample are improved depending on the time and the temperature of the treatment. (Figure 2b). Obviously, the reference sample (pBuA covalently cross-linked) does not exhibit any healing properties after damage at room temperature, neither at higher temperature. A standard stress/strain tensile experiment shows a significant recovery of tensile strength at break (0.15 MPa) and elongation at break (1400%, *ie.* 75 % of the original value) for a sample which has been healed at 90°C (Figure 2c). The SEM picture of a damaged/healed area illustrates the high quality of the healing process (Figure 3c).

Figure 2. a) DMTA traces of pBuA crosslinked by covalent bonds and by the tin oxo-cluster, b) Evolution of the elongation at break as a function of the temperature and the time of heating applied on the sample after damage c) stress-strain tensile curves for undamaged and damaged/healed hybrid pBuA.

Figure 3. a) bisected monolithic sample, b) healed sample, c) SEM observation of the healed sample.

In the context of (self)-healing materials, polymers and composites are currently by far the most attractive and studied class of materials. Accordingly, different approaches to built self-healing polymers have been recently described^{1-4, 24, 25} Especially, repeated healing processes can be achieved with systems based on reversible systems, that either uses covalent^{26, 27} and non-covalent bonds, mainly involving supramolecular chemistry based on hydrogen-bonding and metal coordination

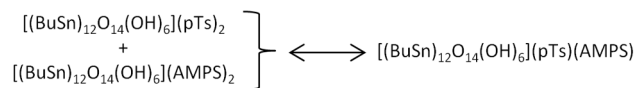
chemistry.²⁸⁻³⁰ In our sample, the ionic bonds at the hybrid interface are more labile and have the ability to be broken and reformed compared with all the covalent bonds of the main chain; the re-distribution of the ionic bonds is likely the major reason for the observed behavior. To highlight the dynamic nature of the cross-links nodes, a piece of material made of n-BuA copolymerized with 6 wt% of [(BuSn)₁₂O₁₄(OH)₆](AMPS)₂ was swollen with a solution of [(BuSn)₁₂O₁₄(OH)₆](pTs)₂ in CDCl₃, the amount of added oxo-clusters being equal to the one already present in the material (pTs: *p*-toluene sulfonate). For comparison, a piece of pBuA covalently cross-linked with 0.17 w% of 1,6-hexanediol dimethacrylate, which contains the same molar amount of cross-links, was also swollen with the solution of [(BuSn)₁₂O₁₄(OH)₆](pTs)₂ in CDCl₃. The ¹¹⁹Sn-(¹H) NMR spectra of these two swollen samples are presented in figure 4. They both exhibit the characteristic ¹¹⁹Sn NMR signature of [(BuSn)₁₂O₁₄(OH)₆]₂ compounds. Compared to the spectrum obtained without the addition of free oxo-clusters (Figure SI1), the resonances are much more narrow, as expected for more mobile species. Yet, the line widths observed for the mendable material remain larger than for the covalently cross-linked elastomer. This feature is in line with an exchange of the additional oxo-clusters with the ones that cross-linked the material.

Figure 4. Zoom on the two resonances of the ¹¹⁹Sn-(¹H) NMR spectra of elastomer samples swollen with a solution of [(BuSn)₁₂O₁₄(OH)₆](pTs)₂ in CDCl₃. a) BuA co-polymerized with 6 w% of [(BuSn)₁₂O₁₄(OH)₆](AMPS)₂ b) BuA co-polymerized with 0.17 w% of 1,6-hexanediol dimethacrylate.

To further prove this exchange, PFG (Pulsed Field Gradient) NMR experiments were performed³¹ using the ¹H signals of the pTs anions (around 7 ppm), which are not hidden below the intense signals of pBuA, and the ¹¹⁹Sn signal of the six-coordinated tin atoms of the oxo-clusters (-463 ppm); the ¹H signals related to the butyltin oxo-core being hidden by the pBuA signals. The attenuation profiles, measured with both experiments on each samples, are presented in Figure 5. They are plotted as ln(I/I₀) vs. (γgδ)²(Δ-δ/3), where γ is the gyromagnetic ratio, g the gradient strength (including the gradient shape factor), δ the equivalent gradient pulse length, and Δ the diffusion delay. For the covalently cross-linked material (Figure 5a), both PFG NMR measurements (*i.e.* ¹H and ¹¹⁹Sn) yield the same diffusion coefficient (*i.e.* same slope). This observation agrees perfectly with the non-dissociation of [(BuSn)₁₂O₁₄(OH)₆]₂ compounds in solvents with low dielectric constants (such as CDCl₃)^{32, 33}. The diffusion is yet slower than in pure CDCl₃ (2.5 10⁻¹⁰ vs. 4.9 10⁻¹⁰ m²s⁻¹)[†], likely because of the hindrance related to the tortuosity of the swollen network. On the contrary, for the sample cross-linked with [(BuSn)₁₂O₁₄(OH)₆](AMPS)₂, clearly different diffusion coefficients are obtained from ¹H and ¹¹⁹Sn PFG NMR measurements; the apparent diffusion coefficient of the macrocations being half of the one of the anions (0.4 10⁻¹⁰ vs

0.8 10⁻¹⁰ m²s⁻¹) (Figure 5b). Such a difference, in a solvent where the ionic dissociation of [(BuSn)₁₂O₁₄(OH)₆]₂ compounds does not take place, [†] can be explained by fast exchange reactions between the added oxo-clusters and the cross-links nodes.

This exchange is schematised in figure 5c and can be summarized as follow:



where AMPS stands for a 2-acrylamido-2-methyl-1-propanesulfonate anion which has co-polymerized with the BuA. For fast exchange regime, the apparent diffusion coefficient equal the molar fraction weighted average of the diffusion coefficients of the different species. Yet, in the present case, among the three possible species present at equilibrium, only [(BuSn)₁₂O₁₄(OH)₆](pTs)₂ is able to diffuse freely (diffusion coefficient = D_F). The two others are bound to the network by one, [(BuSn)₁₂O₁₄(OH)₆](AMPS)(pTs), or two, [(BuSn)₁₂O₁₄(OH)₆](AMPS)₂, of their anions and their diffusion coefficients are zero (or negligible compared to D_F). Accordingly, the apparent diffusion coefficients of the pTs and the oxo-clusters can be written:

$$D_{app}(pTs) = f(\text{mobile pTs}) \times D_F$$

and

$$D_{app}(\text{oxo-cluster}) = f(\text{mobile oxo-cluster}) \times D_F$$

The studied sample containing initially the same amount of [(BuSn)₁₂O₁₄(OH)₆](pTs)₂ and [(BuSn)₁₂O₁₄(OH)₆](AMPS)₂, the equilibrium molar fraction of each species is 1/3, if one makes the reasonable assumption that the affinity of the macrocation is identical for both anions (both are sulfonates). Therefore, at equilibrium, the fraction of pTs in a species able to diffuse is 2/3, while the fraction of oxo-cluster in a species able to diffuse is only 1/3. Accordingly, D_{app}(pTs) equals two thirds of D_F and D_{app}(oxo-cluster) equals only one third of D_F. The theoretical ratio of these two apparent diffusion coefficients agrees perfectly with the ratio experimentally determined with ¹H or ¹¹⁹Sn PFG NMR. Moreover, D_F can also be estimated at 1.2 10⁻¹⁰ m²s⁻¹. This value is *ca.* half of the one measured in the covalently cross-linked network. The difference might arise from different network inner structures, despite the fact that they have both the same cross-linking density. It can also be related to a slightly different swelling ratio, which is difficult to precisely control inside the 5 mm NMR tube. These measurements confirm the ability of [(BuSn)₁₂O₁₄(OH)₆]₂²⁺ based cross-linking nodes to take part in fast exchange reactions, that can redistribute the bonding network and play a major role for the self-healing properties.

Figure 5. PFG NMR attenuation profiles (^1H : empty circles, ^{119}Sn : filled circles) obtained on elastomer samples swollen with a solution of $[(\text{BuSn})_{12}\text{O}_{14}(\text{OH})_6](\text{pTs})_2$ in CDCl_3 a) BuA co-polymerized with 6 w% of $[(\text{BuSn})_{12}\text{O}_{14}(\text{OH})_6](\text{AMPS})_2$ (the amount of added $[(\text{BuSn})_{12}\text{O}_{14}(\text{OH})_6](\text{pTs})_2$ match the amount of originally present $[(\text{BuSn})_{12}\text{O}_{14}(\text{OH})_6](\text{AMPS})_2$ b) BuA co-polymerized with 0.17 w% of 1,6-hexanediol dimethacrylate c) Schematic of the exchange of $[(\text{BuSn})_{12}\text{O}_{14}(\text{OH})_6](\text{AMPS})_2$ (blue links) with $[(\text{BuSn})_{12}\text{O}_{14}(\text{OH})_6](\text{pTs})_2$ (green links).

Accordingly, due to the specific nature of the cross-linkers, when two pieces of sample are set together, the dynamic behavior of the material allows the diffusion of the clusters and the macromolecules moieties at the mesoscale, which results into a macroscopic effect. Consequently, the healing of cracks or fractures is observed at room temperature without the need of an external stimulus. Upon increasing the temperature the healing process is speed up in agreement with the dynamic behavior of the system and the ability of the cross-linkers to move inside the elastomeric matrix. Moreover, such hybrid materials can be reversibly deformed or processed in a stable shape under stress after few days at room temperature or more faster by heating few minutes at 120°C . The deformed shape obtained is illustrated in figure 6.

Figure 6. a) initial sample, b) sample deformed at room temperature

Conclusions

In summary, the NBBs have multiple impacts on the polymer. This bioinspired strategy is based on the incorporation of sacrificial and reversible cross-links into polymers,⁶ and leads to the design of smart materials. This new family of ionomers,³⁴ containing a very low amount of ionic species, yield to materials with the ability to self-repair themselves after a strong damage. The process is fully reversible and allows the design of materials with a combination of properties. As a conclusive outlook, the simplicity of the chemistry presented is versatile, relies on readily available organic monomers, and does not require any special polymerization procedure. Consequently it well-matches with the synthesis of daily life polymers. The strategy presently described to produce reparable networks could potentially be generalized to various other polymerization schemes and be extended to other NBBs for long-life or durable plastics or rubbers. Hybridization of polymers offers the opportunity to extent lifetimes of materials but it can also bring additional multifunctionalities according to the wealth of properties offered by the inorganic components (mechanical enhancement, thermal stability, magnetism, optic, etc...).

Experimental

All the chemical products are commercially available and were used as received without further purification. n-Butyl acrylate was purchased from Acros Organics, n-butylin hydroxide oxide hydrate purchased from Strem Chemicals, 2-Acrylamido-2-methyl-1-propanesulfonic acid (AMPSH) from Aldrich, Azobisisobutyronitrile (AIBN) from Fluka.

Tin cluster, $[(\text{BuSn})_{12}\text{O}_{14}(\text{OH})_6](\text{AMPS})_2$ was synthesized as described by Ribot and al.²²

Hybrid material was synthesized from a mixture of 2%wt of Tin clusters in n-butyl acrylate. n-Butyl acrylate was first out gazed by a bubbling of argon. Then, the Tin cluster and the radical initiator (AIBN) were added. Typically, for 6 mL of n-butyl acrylate, 107 mg of Tin clusters (2% in weight) and 138 mg of AIBN (2 mol % of the total amount of polymerizable functions) were added. The solution, ready to polymerize, was then transferred with a syringe into a mold made of a silicon seal in between two glass plates. The filled mold was then placed in a water bath at 60°C for ~15 hours.

Dynamic Mechanical Analysis experiments were conducted on a DMA Tritec from BOHLIN in the tension geometry. Heating ramp of $2^\circ\text{C}/\text{min}$ were applied from -80°C to 40°C . Rectangular samples of 5.25 mm length and 6.2mm*3.3mm cross section were tested at 1Hz and 1% of amplitude.

Tensile tests experiments were performed at room temperature on dogbone sample (30mm*5mm*2mm) using a Instron 4507 tensile machine with a strain rate of 10 mm/min. The tests were performed up to the break of each sample.

NMR experiments were performed on a Bruker Avance^{III} 300 spectrometer (300.13 MHz for ^1H and 111.92 MHz for ^{119}Sn) using a 5 mm ^1H -X BBFO probe equipped with a z-gradient coil able to provide a maximum gradient strength of 49.8 Gcm^{-1} . All experiments were carried out at 25°C . ^1H PFG NMR experiments were performed with a stimulated echo pulse sequence using a longitudinal eddy current delay (5 ms), bipolar gradient pulses and two spoil gradient pulses (ledbpgp2s).³⁵ All the gradient pulses were sine-shaped. Attenuation profiles were measured with 32 gradient values, linearly spaced between 2 and 90% of the maximum gradient strength. 32 transients were summed for each gradient value. For each sample, at least four experiments, using different sets of diffusion delay and gradient pulse length ($\square, \square\square$), were run to check for the absence of convection (as expected for a diffusion in an swollen elastomer). All the ($\square, \square\square$) pairs used yielded an attenuation stronger than 95% for the higher gradient strength. These multiple measures also showed that the dispersion of the D values is lower than 5%. ^{119}Sn PFG NMR was performed with a stimulated echo sequence using an INEPT polarisation transfer, bipolar gradient pulses, one spoil gradient pulse and decoupling during acquisition (stebpgp1s).³⁶ The use of a such a sequence has two main advantages: the signal intensity is increased and, more interestingly, the phase

coding and decoding gradient pulses act on the ^1H magnetization, thus avoiding the classical limitation in heteronuclear detected PFG NMR experiments associated to low gyromagnetic ratios. The gradient pulses were sine-shaped, the spectral window was centred on the six-coordinate tin atom signal (-463 ppm) and a J coupling of 140 Hz was used (optimized with INEPT experiments). For ^{119}Sn , the attenuation profile was determined with 12 gradient values, linearly spaced between 2 and 90% of the maximum gradient strength. 5120 transients were summed for each gradient value. According to the length of the experiment (~54 hrs), only one set of diffusion delay and gradient pulse length ($\square=350$ ms and $\square\square=1.6$ ms) was selected. It yielded a maximum attenuation of 55 and 90%, for BuA co-polymerized with 6 w% of $[(\text{BuSn})_{12}\text{O}_{14}(\text{OH})_6](\text{AMPS})_2$ and BuA co-polymerized with 0.17 w% of 1,6-hexanediol dimethacrylate, respectively. ^1H and ^{119}Sn PFG NMR experiments were analysed with TOPSPIN 3.1 (Bruker).

Notes and references

^a Sorbonne Universités, UPMC Univ Paris 06, UMR 7574, Chimie de la Matière Condensée de Paris, F-75005, Paris, France.

^b CNRS, UMR 7574, Chimie de la Matière Condensée de Paris, F-75005, Paris, France.

^c Collège de France, UMR 7574, Chimie de la Matière Condensée de Paris, F-75005, Paris, France.

^d Arts et Métiers ParisTech, Laboratoire PIMM, F-75013, Paris, France.

^e PSA Peugeot Citroën, F-78943 Vélizy Villacoublay, France.

† The diffusion coefficient of $[(\text{BuSn})_{12}\text{O}_{14}(\text{OH})_6](\text{pTs})_2$ in CDCl_3 (2.7 w%) was independently measured by ^1H PFG NMR. Such measures, in which the pTs anions and the butyltin oxo-core can be both followed, also confirmed the absence of ionic dissociation (*i.e.* the anions and macrocation exhibit the same diffusion coefficient)./

- M. D. Hager, P. Greil, C. Leyens, S. van der Zwaag and U. S. Schubert, *Adv. Mater.*, 2010, 22, 5424-5430.
- S. D. Bergman and F. Wudl, *J. Mater. Chem.*, 2008, 18, 41-62.
- K. A. Williams, D. R. Dreyer and C. W. Bielawski, *Mrs Bulletin*, 2008, 33, 759-765.
- J. P. Youngblood, N. R. Sottos and C. Extrand, *Mrs Bulletin*, 2008, 33, 732-741.
- M. J. Harrington, A. Masic, N. Holten-Andersen, J. H. Waite and P. Fratzl, *Science*, 2010, 328, 216-220.
- S. Krauss, T. H. Metzger, P. Fratzl and M. J. Harrington, *Biomacromolecules*, 2013, 14, 1520-1528.
- L. Nicole, L. Rozes and C. Sanchez, *Adv. Mater.*, 2010, 22, 3208-3214.
- C. Sanchez, P. Belleville, M. Popall and L. Nicole, *Chem. Soc. Rev.*, 2011, 40, 696-753.
- G. Kickelbick, *Prog. Polym. Sci.*, 2003, 28, 83-114.
- C. Sanchez, B. Lebeau, F. Chaput and J. P. Boilot, *Adv. Mater.*, 2003, 15, 1969-1994.
- F. Mammeri, E. Le Bourhis, L. Rozes and C. Sanchez, *J. Mater. Chem.*, 2005, 15, 3787-3811.
- C. Sanchez, C. Boissiere, D. Grosso, C. Laberty and L. Nicole, *Chem. Mater.*, 2008, 20, 682-737.
- C. Sanchez, H. Arribart and M. M. G. Guille, *Nat. Mater.*, 2005, 4, 277-288.
- S. Kango, S. Kalia, A. Celli, J. Njuguna, Y. Habibi and R. Kumar, *Prog. Polym. Sci.*, 2013, 38, 1232-1261.
- U. Schubert, *Chem. Mater.*, 2001, 13, 3487-3494.
- U. Schubert, *Chem. Soc. Rev.*, 2011, 40, 575-582.
- C. Sanchez, G. Soler-Illia, F. Ribot, T. Lalot, C. R. Mayer and V. Cabuil, *Chem. Mater.*, 2001, 13, 3061-3083.
- L. Rozes and C. Sanchez, *Chem. Soc. Rev.*, 2011, 40, 1006-1030.
- W. A. Zhang and A. H. E. Muller, *Prog. Polym. Sci.*, 2013, 38, 1121-1162.
- L. Rozes, G. Fornasieri, S. Trabelsi, C. Creton, N. E. Zafeiropoulos, M. Stamm and C. Sanchez, *Progress in Solid State Chemistry*, 2005, 33, 127-135.
- F. Périneau, S. Pensec, C. Sassoie, F. Ribot, L. Van Lokeren, R. Willem, L. Bouteiller, C. Sanchez and L. Rozes, *J. Mater. Chem.*, 2011, 21, 4470-4475.
- F. Ribot, D. Veautier, S. J. Guillaudeu and T. Lalot, *J. Mater. Chem.*, 2005, 15, 3973-3978.
- A. Strachota, F. Ribot, L. Matejka, P. Whelan, L. Starovoytova, J. Plestil, M. Steinhart, M. Slouf, J. Hromadkova, J. Kovarova, M. Spirkova and B. Strachota, *Macromolecules*, 2012, 45, 221-237.
- S. R. White, N. R. Sottos, P. H. Geubelle, J. S. Moore, M. R. Kessler, S. R. Sriram, E. N. Brown and S. Viswanathan, *Nature*, 2001, 409, 794-797.
- J. L. Yang, M. W. Keller, J. S. Moore, S. R. White and N. R. Sottos, *Macromolecules*, 2008, 41, 9650-9655.
- X. X. Chen, M. A. Dam, K. Ono, A. Mal, H. B. Shen, S. R. Nutt, K. Sheran and F. Wudl, *Science*, 2002, 295, 1698-1702.
- A. Rekondo, R. Martin, A. Ruiz de Luzuriaga, G. Cabanero, H. J. Grande and I. Odriozola, *Materials Horizons*, 2014, DOI: 10.1039/c3mh00061c.
- J. Fox, J. J. Wie, B. W. Greenland, S. Burattini, W. Hayes, H. M. Colquhoun, M. E. Mackay and S. J. Rowan, *J. Am. Chem. Soc.*, 2012, 134, 5362-5368.
- P. Cordier, F. Tourmilhac, C. Soulie-Ziakovic and L. Leibler, *Nature*, 2008, 451, 977-980.
- F. Perineau, S. Pensec, C. Sanchez, C. Creton, L. Rozes and L. Bouteiller, *Polymer Chemistry*, 2011, 2, 2785-2788.
- P. T. Gallagher, *Translational Dynamics & Magnetic Resonance - Principles of Pulsed Gradient Spin Echo NMR*, Oxford University Press, Oxford, 2011.
- L. Van Lokeren, G. Maheut, F. Ribot, V. Escax, I. Verbruggen, C. Sanchez, J. C. Martins, M. Biesemans and R. Willem, *Chem.-Eur. J.*, 2007, 13, 6957-6966.
- L. Van Lokeren, R. Willem, D. van der Beek, P. Davidson, G. A. Morris and F. Ribot, *Journal of Physical Chemistry C*, 2010, 114, 16087-16091.
- S. J. Kalista, in *Self-healing Materials: Fundamentals, Design strategies and Applications*. Eds Swapna Kumar Ghosh; WILEY-VCH Verlag GmbH & Co. KGaA, Weinheim, 2009.

35. D. H. Wu, A. D. Chen and C. S. Johnson, *Journal of Magnetic Resonance Series A*, 1995, 115, 260-264.
36. D. H. Wu, A. D. Chen and C. S. Johnson, *Journal of Magnetic Resonance Series A*, 1996, 123, 215-218.

Figure caption:

Figure 1. Schematic representation of the hybridization of the polymer by the butyltin oxo-cluster macrocation, $[(\text{BuSn})_{12}\text{O}_{14}(\text{OH})_6]^{2+}$, functionalized through ionic interactions with two charge compensating acrylamide anions.

Figure 2. a) DMTA traces of pBuA crosslinked by covalent bonds and by the tin oxo-cluster, b) Evolution of the elongation at break as a function of the temperature and the time of heating applied on the sample after damage c) stress-strain tensile curves for undamaged and damaged/healed hybrid pBuA.

Figure 3. a) bisected monolithic sample, b) healed sample, c) SEM observation of the healed sample.

Figure 4. Zoom on the two resonances of the ^{119}Sn -(^1H) NMR spectra of elastomer samples swollen with a solution of $[(\text{BuSn})_{12}\text{O}_{14}(\text{OH})_6](\text{pTs})_2$ in CDCl_3 . a) BuA co-polymerized with 6 w% of $[(\text{BuSn})_{12}\text{O}_{14}(\text{OH})_6](\text{AMPS})_2$ b) BuA co-polymerized with 0.17 w% of 1,6-hexanediol dimethacrylate.

Figure 5. PFG NMR attenuation profiles (^1H : empty circles, ^{119}Sn : filled circles) obtained on elastomer samples swollen with a solution of $[(\text{BuSn})_{12}\text{O}_{14}(\text{OH})_6](\text{pTs})_2$ in CDCl_3 a) BuA co-polymerized with 6 w% of $[(\text{BuSn})_{12}\text{O}_{14}(\text{OH})_6](\text{AMPS})_2$ (the amount of added $[(\text{BuSn})_{12}\text{O}_{14}(\text{OH})_6](\text{pTs})_2$ match the amount of originally present $[(\text{BuSn})_{12}\text{O}_{14}(\text{OH})_6](\text{AMPS})_2$ b) BuA co-polymerized with 0.17 w% of 1,6-hexanediol dimethacrylate c) Schematic of the exchange of $[(\text{BuSn})_{12}\text{O}_{14}(\text{OH})_6](\text{AMPS})_2$ (blue links) with $[(\text{BuSn})_{12}\text{O}_{14}(\text{OH})_6](\text{pTs})_2$ (green links).

Figure 6. a) initial sample, b) sample deformed at room temperature

FIG 1

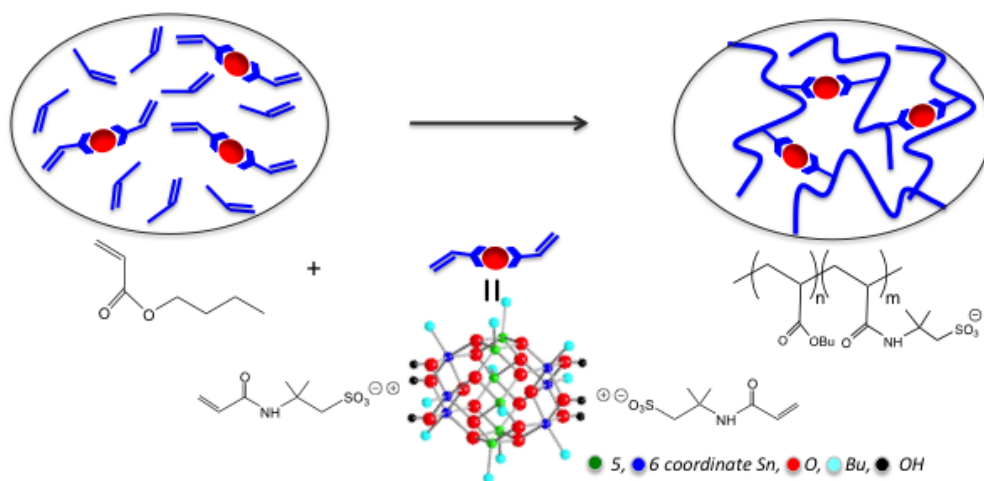


FIG2

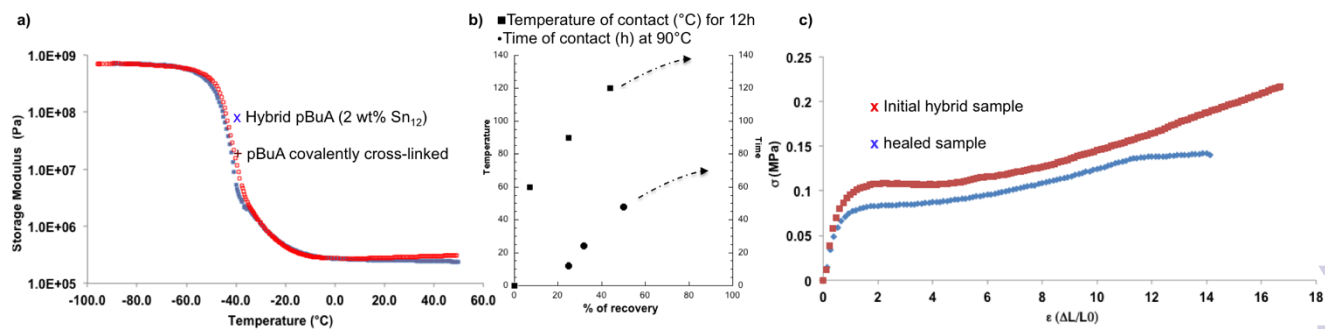


FIG3

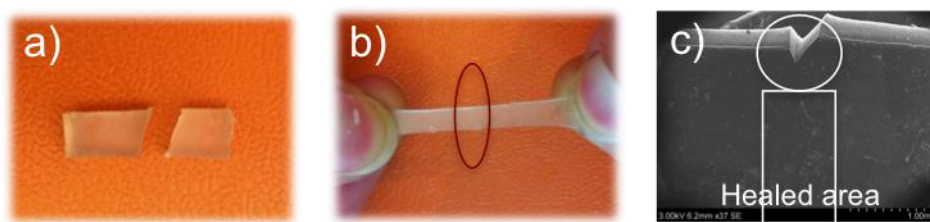


FIG4

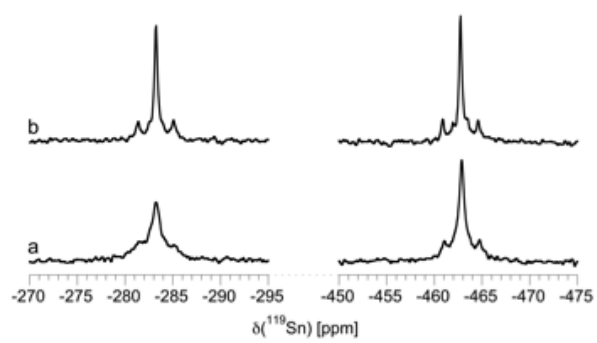


FIG5

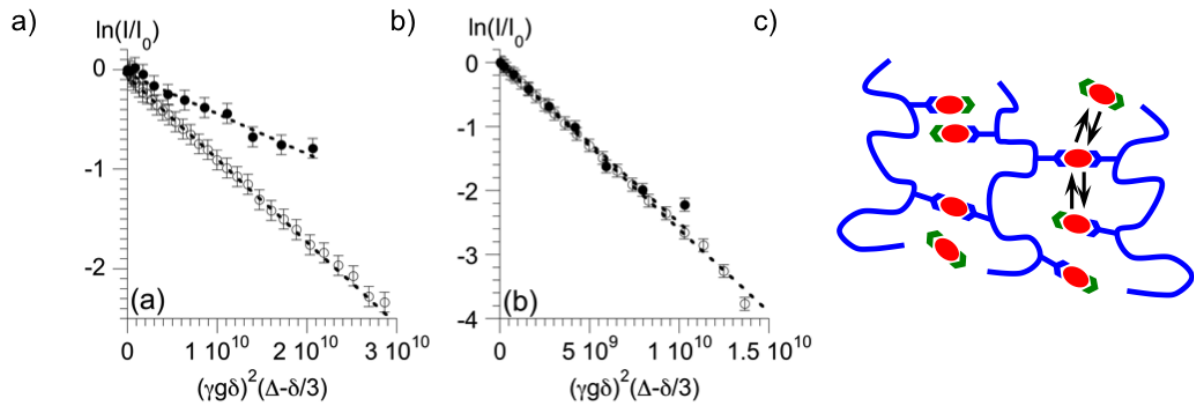


FIG6

